11084 *Biochemistry* **2009,** *48,* 11084–11096
DOI: 10.1021/bi900649t

BIOCHEMISTRY
including biophysical chemistry & molecular biology
Article

Mechanisms of Protein Stabilization and Prevention of Protein Aggregation by Glycerol[†]

Vincent Vagenende,[‡,§] Miranda G. S. Yap,[‡,§] and Bernhardt L. Trout*[,‡,∥]

[‡]*Singapore-MIT Alliance, National University of Singapore, 4 Engineering Drive 3, Singapore 117576,* [§]*Bioprocessing Technology Institute, 20 Biopolis Way #06-01, Centros, Singapore 138668, and* [∥]*Department of Chemical Engineering, Massachusetts Institute of Technology, 77 Massachusetts Avenue, Cambridge, Massachusetts 02139*

Received April 15, 2009; Revised Manuscript Received October 7, 2009

ABSTRACT: The stability of proteins in aqueous solution is routinely enhanced by cosolvents such as glycerol. Glycerol is known to shift the native protein ensemble to more compact states. Glycerol also inhibits protein aggregation during the refolding of many proteins. However, mechanistic insight into protein stabilization and prevention of protein aggregation by glycerol is still lacking. In this study, we derive mechanisms of glycerol-induced protein stabilization by combining the thermodynamic framework of preferential interactions with molecular-level insight into solvent−protein interactions gained from molecular simulations. Contrary to the common conception that preferential hydration of proteins in polyol/water mixtures is determined by the molecular size of the polyol and the surface area of the protein, we present evidence that preferential hydration of proteins in glycerol/water mixtures mainly originates from electrostatic interactions that induce orientations of glycerol molecules at the protein surface such that glycerol is further excluded. These interactions shift the native protein toward more compact conformations. Moreover, glycerol preferentially interacts with large patches of contiguous hydrophobicity where glycerol acts as an amphiphilic interface between the hydrophobic surface and the polar solvent. Accordingly, we propose that glycerol prevents protein aggregation by inhibiting protein unfolding and by stabilizing aggregation-prone intermediates through preferential interactions with hydrophobic surface regions that favor amphiphilic interface orientations of glycerol. These mechanisms agree well with experimental data available in the literature, and we discuss the extent to which these mechanisms apply to other cosolvents, including polyols, arginine, and urea.

Since proteins are only marginally stable, preserving their stability and activity in biological and biotechnological applications can pose serious challenges. Although protein stability is routinely enhanced via addition of cosolvents such as salts, amino acids, and polyols (*1*, *2*), the mechanisms by which cosolvents induce protein stability remain elusive. Enhancement of protein stability by cosolvents is generally related to the shift of protein conformations toward more compact and ordered sates (*3*) and the inhibition of partial unfolding leading to protein aggregation (*4*, *5*). In fact, protein aggregation has been recognized as a major manifestation of instability that can severely affect protein functionality in vivo and in vitro (*6*−*10*). In addition, there has been a growing awareness of the importance of the conformational space of native proteins for protein catalysis (*11*), protein−protein interactions (*12*), and protein folding (*13*). Like protein stability, the conformational space and the energy landscape of the protein (*14*) depend on the solvent conditions of the protein solution (*11*). Thus, mechanistic insight into effects of cosolvents on the conformational space and stability of proteins is desired for the understanding and design of protein processes pertinent to biology and biotechnology.

Among the cosolvents most widely used to stabilize proteins are polyols (*15*−*17*). Protein stabilization and compaction by polyols (*3*, *18*−*23*) have been attributed to mechanisms such as the excluded volume effect (*1*, *5*, *24*) and the solvophobic effect (*25*), which lead to protein conformations with minimal solvent accessible surface area. By the same mechanisms, polyols would promote reversible protein association because the solvent accessible surface area of the protein complex is smaller than that for unassociated proteins (*26*). However, polyols promote protein association for only some protein complexes but not for others (*27*−*30*). Polyols are also effective in preventing protein aggregation during refolding of many proteins (*31*−*33*) and are frequently included in solvent screens to optimize the refolding yield of recombinant proteins (*34*). Strikingly, the effectiveness of polyols in preventing protein aggregation varies widely among different polyols, yet the underlying reasons are not understood (*31*). Besides, polyols can cause local conformational changes leading to increased flexibility of certain protein segments (*35*−*37*). Evidently, plausible mechanisms for explaining polyol-induced protein compaction should also account for these effects.

One of the most widely used polyols to stabilize proteins is glycerol (*38*−*42*). Glycerol is routinely used in protein refolding (*31*), protein crystallization (*43*), formulation of biopharmaceuticals, (*6*) and in the food industry (*44*). Glycerol induces protein compaction (*20*, *21*, *23*), reduces protein flexibility (*22*, *45*), stabilizes specific partially unfolded intermediates (*26*, *45*−*48*), and affects both native and non-native protein aggregation (*5*, *27*−*29*), including protein amyloidogenesis (*49*). The widespread use of glycerol stands in sharp contrast with the lack of mechanistic insight into the effects of glycerol on protein stability and aggregation. Therefore, we believe that insight into the effects of glycerol on protein stability and aggregation would benefit protein-related research and

[†]Funding support provided by the Singapore-MIT Alliance.
*To whom correspondence should be addressed. E-mail: trout@mit.edu. Phone: (617) 258-5021. Fax: (617) 253-2272.

 Published on Web 10/09/2009

applications. Moreover, as glycerol is one of the smallest and most simple molecules in the polyol class, we consider a molecular-level study of the effects of glycerol on protein stability and aggregation as a good start in elucidating protein stabilization and protein aggregation mechanisms by polyols.

A thermodynamic framework accounting for the effects of cosolvents on protein thermodynamics is provided by preferential interaction theory (*1*, *25*, *50*−*52*). The effect of cosolvents on the equilibrium between distinct protein conformations can be predicted on the basis of the difference in preferential interaction coefficients between distinct protein conformations. The preferential interaction coefficient for a protein in a cosolvent/water mixture, Γ_{XP},[1] is a measure for the excess number of cosolvent molecules near the protein surface (*53*) and can be measured by experimental techniques such as dialysis densitometry and vapor pressure osmometry (*38*, *54*, *55*). However, quantitative analysis of the effects of cosolvents on protein thermodynamics is difficult because experimental measurements yield only the ensemble average of Γ_{XP} values of the various protein conformations under specific solvent conditions (*56*). As a result, the potential of preferential interaction theory to elucidate the effects of cosolvents on protein thermodynamics and protein stability remains untapped.

Very recently, convergent Γ_{XP} values of proteins in mixed solvents have been obtained from molecular dynamics simulations (*53*, *57*). We found that Γ_{XP} values of hen egg white lysozyme (HEL) in glycerol/water mixtures differed significantly for distinct protein conformations (*53*). These observations prompted us to further investigate the origins and consequences of significant differences in Γ_{XP} in this study. Building on the molecular insight into preferential interaction coefficients of lysozyme in aqueous glycerol gained in our previous study (*53*), we characterize effects of local protein conformational changes on protein solvation and on Γ_{XP} and propose general mechanisms by which conformational changes affect Γ_{XP}. Subsequently, effects of glycerol on the protein energy landscape are estimated on the basis of preferential interaction theory and referenced to experimentally observed effects of glycerol on protein compaction and protein flexibility. Moreover, preferential interactions of glycerol with a hydrophobic surface are characterized, and two mechanisms underlying the inhibition of protein aggregation by glycerol are presented. Finally, we evaluate the extent to which mechanistic insight into effects of glycerol on protein stabilization applies to other cosolvents, in particular polyols.

METHODOLOGY

Calculation of Γ_{XP} from Molecular Dynamics Simulations. Molecular dynamics simulations are performed using CHARMM (*58*) and NAMD (*59*) as described in our previous article (*53*). All simulations comprise hen egg white lysozyme (HEL) in a solvent box. For Sim U5, the solvent is pure water; for Sim C1 and Sim C2, the solvent is 17% (v/v) and 38% (v/v) aqueous glycerol, respectively, and for all other simulations, the solvent is 30% (v/v) aqueous glycerol. Seven simulations (Sim U1−U5, Sim C1, and Sim C2) are run with unconstrained protein coordinates, five simulations (Sim B1−B5) with constrained coordinates of the protein backbone, and two simulations with fixed protein coordinates (Sim F1 and Sim F2). The reference structure for protein constraining is either the crystal structure of PDB entry 194L (Sim B1 and Sim F1) or the structure sampled at 5 ns (Sim B2 and Sim F2), 7 ns (Sim B3), 10 ns (Sim B4), or 21 ns (Sim B5) during Sim U1. To investigate effects of electrostatic interactions on Γ_{XP}, solvent−protein electrostatic interactions are switched off for one simulation (Sim E1) and all electrostatic interactions are switched off for another simulation (Sim E2). Simulation details are listed in Table S1 (Supporting Information).

The preferential interaction coefficient Γ_{XP} is calculated as explained previously (*53*). Practically, Γ_{XP} is determined by the number of glycerol and water molecules within 5 Å of the protein van der Waals surface:

$$\Gamma_{XP} \cong \left\langle n_{XP}(r < 5\text{Å}) - \frac{n_X - n_{XP}(r < 5\text{Å})}{n_W - n_{WP}(r < 5\text{Å})} n_{WP}(r < 5\text{Å}) \right\rangle_{\tau_{run}} \quad (1)$$

where the term in broken brackets refers to the average over the simulation time τ_{run}. The solvent region between 0 Å and 5 Å from the protein van der Waals surface is termed the local domain, and the solvent region for which $r > 5$ Å is the bulk domain. In eq 1, $n_{XP}(r < 5$ Å$)$ and $n_{WP}(r < 5$ Å$)$ are the number of glycerol and water molecules, respectively, in the local domain and n_X and n_W are the total number of glycerol and water molecules, respectively, in the simulation box. The number density ratio $[n_X - n_{XP}(r < 5$ Å$)]/[n_W - n_{WP}(r < 5$ Å$)]$ is fairly constant for all simulations performed in this study (∼0.1065). As a consequence, values of $n_{XP}(r < 5$ Å$)$ and $n_{WP}(r < 5$ Å$)$ that result in the same Γ_{XP} value approximately fall on the line

$$n_{XP}(r < 5\text{Å}) \cong 0.1065 n_{WP}(r < 5\text{Å}) + \Gamma_{XP} \quad (2)$$

Preferential Hydration of Volume Increments of the Local Domain. Over the course of a simulation, the volume of the local domain of the protein generally increases with respect to the local domain of the crystal structure. Increments of the average volumes of solvent regions $[r, r + 0.1$ Å$]$ between two different simulations are calculated in the local domain ($0 < r <$ 5 Å) and termed volume increments, $\Delta V(r)$. To quantify the degree of preferential hydration of volume increments $\Delta V(r)$, the local increase in the number of water molecules $[\Delta n_{WP}{}^{100\%W}(r)]$ is calculated assuming that $\Delta V(r)$ is exclusively occupied by water molecules. Under this assumption, $\Delta n^{wp100\%W}(r)$ equals the product of volume increment $\Delta V(r)$ and local water concentration $c^{wp100\%W}(r)$ in the solvent region $[r, r + 0.1$ Å$]$ for a protein in pure water:

$$\Delta n_{WP}^{100\%W}(r) \equiv c_{WP}^{100\%W}(r) \Delta V(r) \quad (3)$$

On the other hand, if $\Delta V(r)$ would be occupied by bulk solvent [i.e., 30% (v/v) glycerol], $\Delta n_{WP}(r)$ would be 70% of $\Delta n_{WP}{}^{100\%W}(r)$. Hence, the ratio $\Delta n^{wp}(r)/\Delta n_{WP}{}^{100\%W}(r)$ allows us to discern between these two cases: at radial distances r at which the ratio is close to 1.0, volume increments $\Delta V(r)$ are predominantly occupied by water; at radial distances r at which the ratio is close to 0.7, volume increments $\Delta V(r)$ are predominantly occupied by bulk solvent.

Structural and Energetic Contributions to Γ_{XP}. To comprehend the physicochemical origins of preferential interactions of glycerol with the protein, contributions of the excluded volume

[1]Abbreviations: 194L, X-ray structure of HEL in the Protein Data Bank; Γ_{XP}, preferential interaction coefficient; HEL, hen egg white lysozyme; rmsd, root-mean-square deviation; *RT*, gas constant multiplied by the temperature; SASA, solvent accessible surface area.

($\Gamma_{XP,EX}$), van der Waals interactions ($\Gamma_{XP,VDW}$), and electrostatic interactions ($\Gamma_{XP,EL}$) are estimated. Contributions of the excluded volume arise from the difference in the molecular size of glycerol and water (*40*, *60*). The excluded volume of a solvent molecule with respect to a protein is generally estimated by assuming that the solvent molecule is a hard sphere with a radius equal to the molecular van der Waals radius (*40*, *60*). We estimate the excluded volumes for glycerol and water as the volumes comprised within the respective radial distances of the first solvation peak [i.e., 2.3 and 1.0 Å (*53*)]. Notably, the difference in the radial distances of the first solvation peaks equals the difference in the molecular van der Waals radii of glycerol and water in the simulations (i.e., 3.1 and 1.8 Å). The excluded volume effect ($\Gamma_{XP,EX}$) is then estimated assuming that the difference in excluded volumes is exclusively occupied by water at the bulk concentration. With c_X, the glycerol concentration in the bulk domain [i.e., 30% (v/v) glycerol], we obtain

$$\Gamma_{XP,EX} = -c_X \int_{1.0\text{Å}}^{2.3\text{Å}} dV(r) \tag{4}$$

For Sim F1, the contribution of van der Waals interactions is estimated on the basis of Sim E2 for which all electrostatic interactions are switched off by subtracting the excluded volume effect:

$$\Gamma_{XP,VDW}^{SimF1} = \Gamma_{XP}^{SimE2} - \Gamma_{XP,EX}^{SimF1} \tag{5}$$

For other simulations, van der Waals contributions are estimated assuming that $\Gamma_{XP,VDW}$ is proportional to the van der Waals solvent accessible surface area (SASA) of the protein:

$$\Gamma_{XP,VDW} = \frac{SASA - SASA_{SimF1}}{SASA_{SimF1}} \Gamma_{XP,VDW}^{SimF1} \tag{6}$$

Finally, the contribution of electrostatic interactions is estimated as the remainder contribution to Γ_{XP}:

$$\Gamma_{XP,EL} = \Gamma_{XP} - \Gamma_{XP,EX} - \Gamma_{XP,VDW} \tag{7}$$

Free Energies of Transfer. When a cosolvent is added to an aqueous protein solution, the chemical potential of the protein μ_P is altered (*1*, *61*):

$$\Delta\mu_{P,tr} = \int_0^{m_X} \left(\frac{\partial\mu_P}{\partial m_X}\right)_{m_P} dm_X \tag{8}$$

$$= -\int_0^{m_X} \left(\frac{\partial\mu_X}{\partial m_X}\right)_{m_P} \left(\frac{\partial m_X}{\partial m_P}\right)_{\mu_X} dm_X \tag{9}$$

where $\Delta\mu_{P,tr}$ is the free energy of transfer of the protein from pure water to an aqueous solution with m_X molal cosolvent. For infinitely dilute protein solutions, $\partial\mu_X/\partial m_X$ approximately equals RT/m_X, as derived from activity data for binary glycerol/water mixtures (*62*, *63*), and the factor $(\partial m_X/\partial m_P)_{m_X}$ equals the preferential interaction coefficient (*53*). Hence, the transfer free energy $\Delta\mu_{P,tr}^{m_P \to 0}$ of an infinitely dilute protein for transfer from pure water to 30% (v/v) glycerol becomes

$$\Delta\mu_{P,tr}^{m_P \to 0} \cong -\int_0^{m_X} \left(\frac{RT}{m_X}\right) \Gamma_{XP}\, dm_X \tag{10}$$

If Γ^{XP} is linear with the respect to glycerol molality m_X, the integral in eq 10 can be solved, and we obtain

$$\Delta\mu_{P,tr}^{m_P \to 0} \cong -RT\Gamma_{XP} \tag{11}$$

Equation 11 shows that the transfer free energy $\Delta\mu_{P,tr}^{m_P \to 0}$ is negatively proportional to Γ^{XP} if the linearity condition is met. The linearity of Γ_{XP} with respect to the glycerol molality has been observed for most proteins in the concentration range from 0 to 40% (v/v) (*38*) and is in accord with the increase in computed Γ_{XP} values with respect to the glycerol molality (Table 1). Such linearity occurs when preferential interactions are governed by protein−solvent interaction affinities that stay constant within the respective concentration range (*60*) and indicates that the characteristics of protein−solvent interactions do not change in the concentration range from 0 to 40% (v/v). In that case, insight into preferential interactions from a series of simulations of HEL in 30% (v/v) aqueous glycerol is valid over the concentration range that comprises glycerol concentrations that are typically used to stabilize proteins in aqueous solution [i.e., 0−40% (v/v) aqueous glycerol].

Table 1: Computed Values of Γ_{XP} for HEL in Aqueous Glycerol[a]

simulation	constraint[b]	Γ_{XP}	simulation	constraint[b]	Γ_{XP}
F1	fix 194L	-7.1 ± 0.8	B1	bb 194L	-5.7 ± 1.3
F2	fix U1:5ns	-3.9 ± 1.2	B2	bb U1:5ns	-2.8 ± 1.2
U1[c]	−	-8.5 ± 1.5	B3	bb:U1:7ns	-6.8 ± 2.4
U2	−	-5.8 ± 1.0	B4	bb U1:10ns	-7.1 ± 1.9
U3	−	-10.1 ± 1.2	B5	bb U1:21ns	-4.0 ± 1.7
U4	−	-9.2 ± 1.0	E1[d]	fix 194L	38.5 ± 1.1
C1[a]	−	-2.3 ± 0.7	E2[d]	fix 194L	-0.8 ± 1.3
C2[a]	−	-11.6 ± 1.3	Exp[e]	−	-11.4 ± 2.85

[a]For all simulation systems, the solvent comprises 30% (v/v) glycerol (5.87 *m*) except for the systems in Sim C1 and Sim C2 which are run at 17% (v/v) (2.89 *m*) and 38% (v/v) (8.54 *m*) glycerol, respectively. [b]Mode of constraint of protein coordinates (fix, all protein coordinates fixed; bb, harmonical constraint of protein backbone coordinates) and the reference structure for constraining coordinates (194L, PDB structure; U1:*x*ns, structure sampled in Sim U1 after *x* ns). [c]Calculation based on the time interval [5 ns, 25 ns]; no convergence was reached for the last 20 ns due to partial unfolding of the protein. [d]For Sim E1, solvent−protein electrostatic interactions are switched off; for Sim E2, all electrostatic interactions are switched off. [e]Experimental Γ_{XP} value for HEL in 30% (v/v) glycerol (*38*).

RESULTS AND DISCUSSION

Conformational Changes of the Protein Backbone Affect Γ_{XP}. For unconstrained simulations, the protein undergoes conformational changes such that the volume of the local domain, $V(0\text{ Å} < r < 5\text{ Å})$, increases with respect to the crystal structure (Figure S1 of the Supporting Information). We find that the sum $\langle n_{WP}(r < 5.\text{Å})\rangle_{1ns} + 4.7\langle n_{XP}(r < 5.\text{Å})\rangle_{1ns}$ is proportional to $V(0\text{ Å} < r < 5\text{ Å})$ (Figure S1 of the Supporting Information). Hence, $\langle n_{WP}(r < 5.\text{Å})\rangle_{1ns} + 4.7\langle n_{XP}(r < 5.\text{Å})\rangle_{1ns}$ is higher for unconstrained simulations than for the simulation in which protein coordinates are constrained with respect to the crystal structure (Sim F1). In fact, we find that for all simulations both $n_{XP}(r < 5\text{ Å})$ and $n_{WP}(r < 5\text{ Å})$ increase with respect to those of Sim F1 (Figure 1). For some simulations, increases in $n_{XP}(r < 5\text{ Å})$ and $n_{WP}(r < 5\text{ Å})$ do not lead to significant changes in Γ_{XP}, whereas for other simulations, Γ_{XP} is significantly higher or lower than in Sim F1 (Figure 1 and Table 1). This indicates that increments of the volume of the local domain with respect to

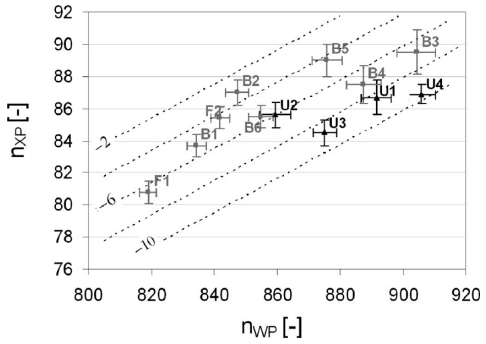

FIGURE 1: Number of glycerol [$n_{XP}(r < 5$ Å)] and water molecules [$n_{WP}(r < 5$ Å)] in the local domain for simulations with unconstrained coordinates (black) and constrained coordinates (gray). Dotted lines indicate iso-Γ_{XP} lines (eq 2) for Γ_{XP} values of −10, −8, −6, −4, and −2.

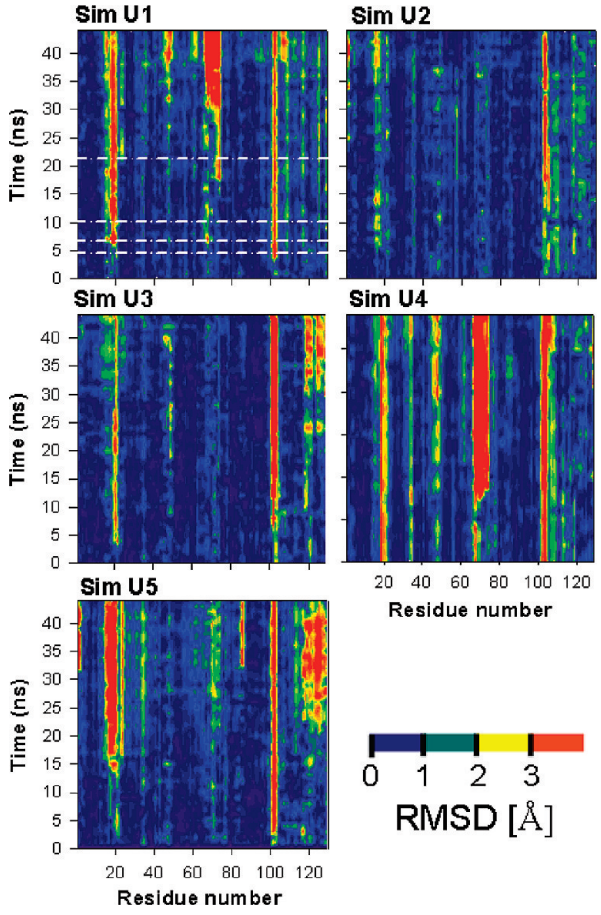

FIGURE 2: Backbone rmsds per residue with respect to the 194L crystal structure. For Sim U1, white lines at 5, 7, 10, and 21 ns indicate the reference structures for Sim B2−B5, respectively.

the crystal structure can be neutrally solvated, preferentially hydrated, or preferentially solvated by glycerol.

The value of Γ_{XP} for a simulation with fixed protein coordinates does not significantly differ from the value of Γ_{XP} for a simulation for which only protein backbone coordinates are constrained with respect to the same reference structure (compare Γ_{XP} values for Sim F1 and Sim B1, as well as Sim F2 and Sim B2 in Table 1). This indicates that the movement of protein side chains does not significantly affect Γ_{XP}. Hence, significant changes in Γ_{XP} must be caused by conformational changes in the protein backbone. The rmsds of backbone residues are plotted in Figure 2.

The rmsds are high (>3 Å) in the loop regions of HEL comprising residues 15−22, 66−74, and 100−103. This corresponds with flexible regions of HEL as evidenced by NMR (*64*) and X-ray crystallography (*65*). Conformational changes in the protein backbone mainly occur during the first 5 ns of each simulation and appear stable at longer simulation times. Notable exceptions are changes for Sim U1 after 25 ns in the loop region of residues 66−74 and changes for Sim U3 and Sim U5 in the N-terminal region. Except for the end of Sim U1, conformational backbone changes appear mostly nativelike (Figure S2 of the Supporting Information).

Protein conformational changes that significantly affect Γ_{XP} occur rapidly. For example, Sim B2 and Sim B3, which are constrained with respect to protein conformations sampled at 5 and 7 ns during Sim U1, give significantly different values of Γ_{XP} (Table 1). Moreover, protein conformational changes are generally transient. This is illustrated by the increase in rmsds (>8 Å) in the loop region of residues 15−22 at 7 ns and the return to average levels (<3 Å) shortly afterward (Figure S2 of the Supporting Information). This is in good agreement with large transient local conformational changes evidenced from hydrogen exchange experiments (*66*). Remarkably, Γ_{XP} for Sim U1 is significantly lower compared to the values of any of the simulations that are constrained with respect to a protein conformation sampled in Sim U1 [Sim B2−B5 (Table 1)]. Thus, the ensemble average of protein conformations resulting in a specific value of Γ_{XP} cannot be replaced by a limited number of representative conformations.

The structural heterogeneity between the protein conformations in 30% (v/v) aqueous glycerol (Sim U1−U4) does not demonstrably differ from the structural heterogeneity of protein conformations in pure water (Sim U5) (Figure 2). Hence, effects of glycerol on the protein conformational space cannot directly be derived from conformational sampling during 40 ns molecular dynamics simulations. Instead, we employ preferential interaction theory to understand the effects of glycerol on protein conformations. Before doing so, we investigate how conformational changes in the protein backbone lead to significant changes in Γ_{XP}.

Conformational Changes Affecting Specific Glycerol−Protein Interactions. For Sim U1, conformational changes in the loop region of residues 66−74 (loop 66−74) (Figure 2) lead to overall increases in temporal values $\langle\Gamma_{XP}\rangle_{\tau_B}$ from 30 ns onward (Figure S3 of the Supporting Information). As a result, Γ_{XP} shifts during the last 20 ns of Sim U1. In the crystal structure, the loop region of residues 66−74 is tightly packed against the rest of the protein (Figure 3A). From 30 ns onward, the loop region is displaced such that a cleft is formed between the loop and the rest of the protein (Figure 3B). The size of the cleft is large, and several solvent accessible N and O atoms of the protein are located inside the cavity. Investigation of the glycerol molecules near the loop region reveals that for the first 30 ns of Sim U1 no glycerol molecules reside longer than 1 ns near loop 66−74. However, after the loop has opened, up to three glycerol molecules concurrently reside in the cleft. Notably, one glycerol molecule resides for 8 ns in the cavity where it forms multiple hydrogen bonds with the protein (Figure 3B). Protein−surface loci where multiple hydrogen bonds with glycerol are formed are called glycerol-binding loci, and solvent regions at such loci positively contribute to Γ_{XP} (*53*). Thus, increases in Γ_{XP} for Sim U1 from 30 ns onward are caused by conformational changes in the

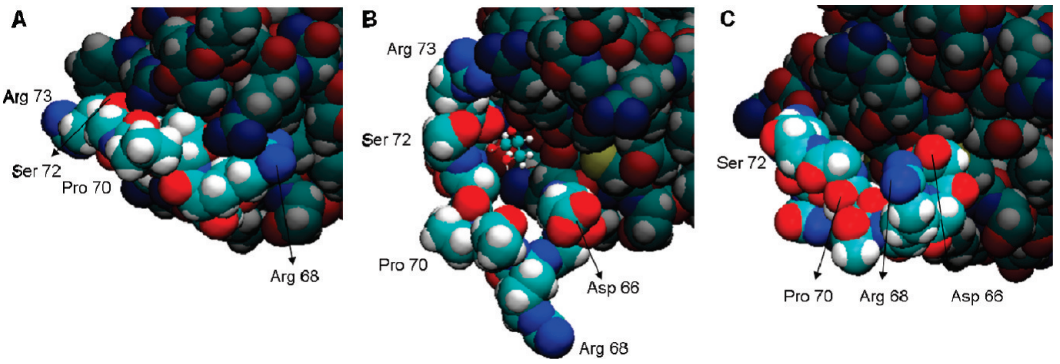

FIGURE 3: van der Waals surface of HEL near residues 66−74 for (A) the minimized crystal structure, (B) Sim U1 at 45 ns, and (C) Sim U4 at 30 ns. Glycerol atoms with residence times of > 5 ns are depicted by ball-and-stick models. Atom types are colored cyan for C, white for H, blue for N, red for O, and yellow for S, and residues 66−74 are highlighted in a brighter shade.

protein backbone leading to the creation of glycerol-binding loci at the protein surface.

Conformational changes in loop 66−74 also occur for Sim U4 (Figure 3C). However, no specific interactions of glycerol molecules with this loop region are observed for Sim U4. We attribute this to the steric exclusion of glycerol from the cleft and the fact that fewer protein N and O atoms are available such that multiple hydrogen bonds with glycerol cannot occur. This is because the cleft between the loop region and the rest of the protein is much smaller for protein conformations in Sim U4 (Figure 3C) compared to Sim U1 (Figure 3B) and because several N and O atoms that are exposed at the protein surface in Sim U1 (Figure 3B) form intramolecular hydrogen bonds in Sim U4 (Figure 3C).

Changes in Γ_{XP} induced by conformational changes in the protein backbone do not correlate with the relative change in the solvent accessible surface area of protein N and O atoms, nor do changes in Γ_{XP} correlate with changes in the surface area of polar, charged, or backbone residues. Arguably, the deficiency in correlations between global protein surface characteristics and preferential interactions arises from the specificity of relative orientations of protein N and O atoms to form multiple hydrogen bonds with glycerol (*53*). This specificity is illustrated by the fact that conformational changes in the same loop region may or may not result in the exposure of glycerol-binding loci at the protein surface (Figure 3).

Preferential Hydration of Volume Increments of the Local Domain. In the previous section, we discussed how conformational changes in the protein affect Γ_{XP} because of the creation or deletion of glycerol-binding loci at the protein surface. Further investigation of the differences in solvation between distinct protein conformations reveals a second mechanism by which conformational changes affect Γ_{XP}. This mechanism generally applies to conformational changes that lead to an increase in the volume of the local solvent domain at the protein surface. We find that, in general, volume increments of the local domain are preferentially hydrated. As a result, Γ_{XP} is lower for expanded conformations compared to compact conformations. This becomes apparent when the solvent composition of the local domain is compared between simulations with unconstrained simulations.

For one simulation with unconstrained coordinates (Sim U2), conformational changes with respect to the crystal structure are limited (Figure 2) and the corresponding value of Γ_{XP} does not change significantly with respect to the crystal structure [Sim F1 (Table 1)], yet for all other unconstrained simulations (Sim U1, Sim U3, and Sim U4), conformational changes in the

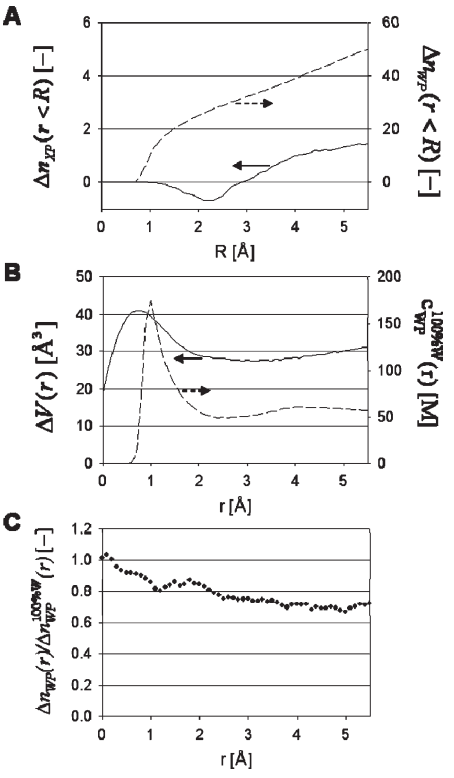

FIGURE 4: Changes in the solvent composition of the local domain upon protein expansion for Sim U4 with respect to Sim U2. (A) Differences in the cumulative number of glycerol, $\Delta n_{XP}(r < R)$, and water, $\Delta n_{WP}(r < R)$, molecules. (B) Volume increments $\Delta V(r, r + 0.1$ Å) and the radial concentration of water $c_{WP}^{100\%W}(r)$ for HEL in pure water. (C) $\Delta n^{WP}(r)/\Delta n_{WP}^{100\%W}(r)$ ratio that is a measure of the degree of preferential hydration of volume increments.

loop region are considerable (Figure 2) and Γ_{XP} is significantly lower with respect to the crystal structure (Table 1). Decreases in Γ_{XP} for Sim U1, Sim U3, and Sim U4 with respect to that for Sim U2 are mainly caused by significant increases in the number of water molecules in the local domain, i.e., $n_{WP}(r < 5$ Å) (Figure 1).

The difference $\Delta n_{WP}(r < 5$ Å) between Sim U4 and Sim U2 results from the continuous increase in $\Delta n_{WP}(r < R)$ from 0.7 Å onward (Figure 4A). In contrast, $\Delta n_{XP}(r < R)$ only starts to increase above 3 Å (Figure 4A). On the basis of volume increments $\Delta V(r)$ and local water concentrations $c_{WP}^{100\%W}(r)$ (Figure 4B), $\Delta n_{WP}^{100\%W}(r)$ is calculated (eq 3). The $\Delta n_{WP}(r)/\Delta n_{WP}^{100\%W}(r)$ ratio gradually decreases and remains constant at 0.7 from 4 Å onward (Figure 4C). Thus, the degree of preferential

Table 2: Structural and Energetic Contributions to Differences $\Delta\Gamma_{XP}$[a]

simulation	$\Delta\Gamma_{XP}$	$\Delta\Gamma_{XP,EX}$	$\Delta\Gamma_{XP,VDW}$	$\Delta\Gamma_{XP,EL}$
U1	−2.7	−0.6	0.0	−2.1
U3	−4.3	−0.2	0.1	−4.1
U4	−3.4	−1.0	0.3	−2.6

[a]Differences with respect to Sim U2.

hydration decreases for increasing radial distances and practically vanishes for r values of >4 Å.

Similarly, volume increments of the local domain for Sim U1 and Sim U3 with respect to Sim U2 are preferentially hydrated near the protein surface. This indicates that conformational changes generally lead to volume increments in the local domain which are preferentially hydrated near the protein surface. Besides, we find that one glycerol molecule in close contact with the protein surface in Sim U2 is replaced with water molecules in Sim U3 (Figure S4 of the Supporting Information). This indicates that conformational changes in Sim U3 not only cause volume increments in the local domain that are preferentially hydrated but also cause the reorientation of protein N and O atoms resulting in the loss of one protein surface locus with a high affinity for glycerol.

Taking together the observations described above, we conclude that the reorientation of protein N and O atoms resulting in the change in glycerol-binding loci may either increase or decrease Γ_{XP} for specific protein conformations. On the other hand, preferential hydration of volume increments generally leads to decreases in Γ_{XP} for expanded protein conformations.

Origins of Preferential Hydration of Volume Increments of the Local Domain. To understand why volume increments in the local domain are generally preferentially hydrated, we investigate the physicochemical origins of preferential interactions. Taking into account the value of Γ_{XP} for Sim E2 (Table 1), we estimate structural and energetic contributions to Γ_{XP} for Sim F1: $\Gamma_{XP,EX}^{\text{Sim F1}} = -21.1$ (eq 4), $\Gamma_{XP,VDW}^{\text{Sim F1}} = 20.3$ (eq 5), and $\Gamma_{XP,EL}^{\text{Sim F1}} = -6.3$ (eq 7). Thus, van der Waals interactions nearly entirely compensate for the excluded volume effect, and the overall value of Γ_{XP} is negative because of the negative contribution of electrostatic interactions. Similar conclusions are drawn for all other simulations. Noteworthy is the fact that the compensation of the excluded volume effect by van der Waals interactions explains why models that account for only the excluded volume (or entropic contributions in general) are not able to predict the effects of glycerol on protein equilibria (*39*, *67*). On the other hand, the correspondence of Γ_{XP} with $\Gamma_{XP,EL}^{\text{Sim F1}}$ explains the success of the electrostatic model of Bolen and coworkers (*68*) for the effects of glycerol on the chemical potential of the protein backbone.

Structural and energetic contributions of differences $\Delta\Gamma_{XP}$ for Sim U1, Sim U3, and Sim U4 with respect to Sim U2 are listed in Table 2. As expected, values of $\Delta\Gamma_{XP,EX}$ are negative because of the expansion of the local domain at radial distances between 1.0 and 2.3 Å (eq 4). Unexpectedly, the protein surface area differs little between different simulations, and therefore, values of $\Delta\Gamma_{XP,VDW}$ are minor (eq 6). However, what is most surprising is that differences in Γ_{XP} are mainly caused by electrostatic interactions. The fact that $\Delta\Gamma_{XP,EL}$ is most negative for Sim U3 corresponds well with the reorientation of protein N and O atoms, leading to the loss of specific glycerol-binding loci as pointed out before, yet values of $\Delta\Gamma_{XP,EL}$ for Sim U1 and Sim U4

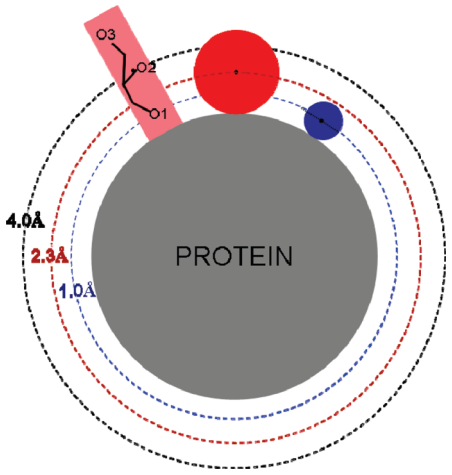

FIGURE 5: Preferential hydration of volume increments mainly results from electrostatic orientation of glycerol at the protein surface. The centers of mass of water (blue circle) and randomly oriented glycerol (red circle) are excluded from the protein van der Waals surface up to radial distances of 1.0 and 2.3 Å, respectively. Notably, the excluded volume effect corresponds with the preferential hydration of the solvent region from 1.0 to 2.3 Å (eq 4). However, because of the electrostatic orientation of glycerol (pink rectangle), glycerol atoms are further excluded from the protein surface and the average exclusion of glycerol molecules is increased to 4.0 Å. Consequently, when the protein expands, volume increments of the solvent region from 1.0 to 4.0 Å are preferentially hydrated.

are also markedly negative. This indicates that electrostatic interactions play a major role in the preferential hydration of volume increments in the local domain near the protein surface.

Electrostatic interactions between solvent molecules and the protein are mostly located at polar atoms of the protein surface, i.e., N and O atoms. This implies that preferential hydration of volume increments mostly occurs at protein N and O atoms (with the exception of N and O atoms at specific glycerol-binding loci). In our previous study (*53*), we showed that glycerol molecules interacting with such protein N and O atoms (i.e., class 1 glycerol molecules) preferentially adopt orientations whereby one of the outer O atoms of glycerol (O1 or O3) is hydrogen-bonded to the protein surface and the vector connecting the hydrogen-bonded O atom with O2 is nearly perpendicular to the protein surface (Figure 5). For such orientations, glycerol atoms are further excluded from the protein surface as would be the case for random orientations of glycerol molecules (Figure 5). On the basis of the calculated values of Γ_{XP} and local volumes $dV(r)$ for Sim U4 and Sim U2, we find that the average exclusion of glycerol molecules from the protein surface is approximately 4.0 Å:

$$\Gamma_{XP}^{\text{SimU4}} - \Gamma_{XP}^{\text{SimU2}} \cong -c_X \int_{1.0\text{Å}}^{4.0\text{Å}} [dV^{\text{SimU4}}(r) - dV^{\text{SimU2}}(r)] \quad (12)$$

This is considerably larger than the excluded volume for randomly oriented glycerol molecules as it is assumed for the calculation of the excluded volume effect [$r < 2.3$ Å (eq 4)]. We conclude therefore that preferential hydration of volume increments of the local domain of a protein in glycerol/water mixtures mainly arises from the electrostatic orientation of glycerol at the protein surface.

Glycerol-Induced Protein Compaction. Remarkably, Γ_{XP} values for Sim U1, Sim U3, and Sim U4 agree well with experiment (Table 1). Hence, we assume that the ensemble

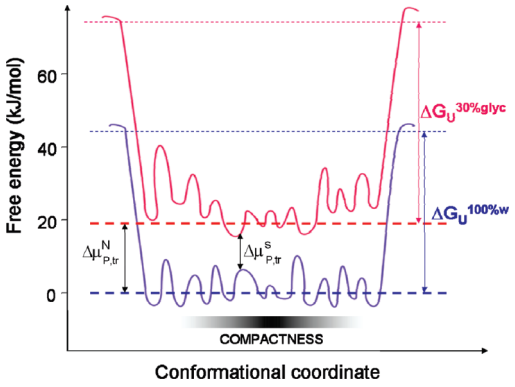

FIGURE 6: Semiquantitative schematic of the energy landscape of native HEL in pure water (blue) and in 30% (v/v) glycerol (red). $\Delta\mu_{P,tr}^{N}$ is the ensemble averaged transfer free energy of native HEL, and $\Delta\mu^{P,trS}$ is the transfer free energy of a specific protein conformation of native HEL. Despite significant differences with respect to the conformational coordinate, values of $\Delta\mu^{P,trS}$ are generally smaller for compact protein conformations. Relative values of the free energy are scaled on the basis of the experimental values of the free energy of unfolding of HEL in pure water ($\Delta G_U^{100\%W} \cong 43$ kJ/mol) and in 30% (v/v) glycerol ($\Delta G_U^{30\%glyc} \cong 53$ kJ/mol) (*94*).

averaged value of Γ_{XP} for native HEL equals the average value of these Γ_{XP} values. The corresponding transfer free energy ($\Delta\mu_{P,tr}^{m_P\rightarrow 0}$) of native HEL from pure water to 30% (v/v) glycerol is approximately 20 kJ/mol (eq 11). In contrast, Γ_{XP} for Sim U2 is significantly higher. We attribute the difference to restricted conformational sampling with a bias toward protein conformations resembling the crystal structure. This is apparent from the agreement between Γ_{XP} of Sim U2 and Γ_{XP} of the crystal structure (Sim F1) and the nonappearance of the experimentally observed conformational disorder in the loop regions of HEL (*64*, *65*) for Sim U2 (Figure 2).

Values of Γ_{XP} for simulations with constrained coordinates (Table 1) correspond with transfer energies ranging form 5 to 20 kJ/mol. The wide range of transfer energies of distinct nativelike protein conformations indicates that glycerol considerably changes the topology of the energy landscape of the native protein (Figure 6). Reorientation of protein N and O atoms between distinct protein conformations altering glycerol-binding loci leads to uneven changes in the energy landscape, whereas preferential hydration of volume increments of the local domain upon protein expansion results in an overall change in the protein energy landscape in favor of compact protein conformations (Figure 6). Considering the importance of protein conformations and dynamics of the native ensemble for protein functionality (*11*−*13*), adequate characterization of glycerol-induced changes in the energy landscape is elementary for understanding the effects of glycerol on protein functionality and protein reactions (*27*−*30*). That is why studies combining molecular dynamics simulations and preferential interaction theory hold untapped potential for comprehension of the effects of glycerol and other cosolvents on protein functionality and protein reactions.

The shift of the native ensemble of HEL to more compact and less flexible conformations in glycerol/water mixtures qualitatively agrees with the experimentally measured decrease in the partial specific volume and the compressibility of HEL in 30% (v/v) glycerol (*20*). Interestingly, Gregory (*22*) attributed the decrease in the hydrogen exchange rate of slowly exchanging amide protons of HEL in the presence of glycerol to the increase in the level of preferential hydration of expanded protein conformations. On the basis of a two-state model, differences in $\Delta\mu_{P,tr}^{m_P\rightarrow 0}$ between expanded and compact protein conformations that agree well with our results were estimated (*22*). In contrast, the hydrogen exchange rate of fast exchanging protons was not affected by preferential hydration. This agrees with our finding that the motion of protein side chains does not significantly affect Γ_{XP}.

Glycerol-induced protein compaction is also observed for other proteins (*21*, *23*, *42*). What is more, protein compaction is also induced by other polyols such as sorbitol (*23*) and sucrose (*18*, *19*). The structural similarity of polyols suggests that the physicochemical origins of preferential hydration of volume increments of the local domain identified for HEL in aqueous glycerol (i.e., electrostatic orientation of glycerol at the protein surface and the excluded volume effect) also cause protein compaction observed for other polyols. The increase in the level of polyol-induced protein compaction with respect to the molecular size of polyols (*23*) can be attributed to the excluded volume effect. In fact, for larger polyols, the excluded volume will be predominantly determined by the molecular size of the polyol. This explains why models that take into account only the molecular size of the polyol are successful for large polyols such as sugars (*67*). However, for smaller polyols, the increase in the excluded volume due to the electrostatic orientation of polyol molecules cannot be disregarded. This is the case for glycerol for which preferential hydration of volume increments mainly originates from the electrostatic orientation of glycerol at the protein surface. Thus, understanding of polyol-induced protein compaction and stabilization requires estimation of the preferential hydration, taking into account the molecular size of the polyol, the electrostatic orientation of polyol molecules at the protein surface, and the volume increments of the local domain upon protein expansion. This importantly adds to the common conception that protein compaction is caused by the excluded volume effect as determined from the molecular size which leads to protein conformations with minimal surface area (*18*, *19*, *24*).

Despite the overall shift toward more compact conformations, polyols can cause local conformational changes leading to increased flexibility of certain protein segments (*35*−*37*). Moreover, effects of glycerol on the local protein flexibility and the chemical potential of a protein depend on the local properties of the protein surface (*42*, *69*). These experimental observations agree with our findings that glycerol is preferentially excluded from most protein surface loci but preferentially bound to certain protein surface loci (*53*). Thus, even though volume increments of the local domain are generally preferentially hydrated, volume increments of some local solvent regions in the local domain may be preferentially solvated. For such solvent regions, glycerol would induce local conformational changes that maximize the volume of these solvent regions.

Preferential Interactions with Hydrophobic Surfaces. Preferential interactions of glycerol with hydrophobic surfaces are investigated by switching off solvent−protein electrostatic interactions (Sim E1). For the hydrophobic surface with the same topology as HEL, water becomes more excluded and glycerol becomes enriched compared to the surface of HEL (Figure 7A). As a result, the preferential interaction coefficient becomes strongly positive for the hydrophobic surface (Table 1). At the hydrophobic surface, glycerol orientations are preferred whereby glycerol C atoms are in direct contact with the hydrophobic surface and O atoms point toward the solvent (Figure 7B). In contrast, relatively few water O atoms make contact with the

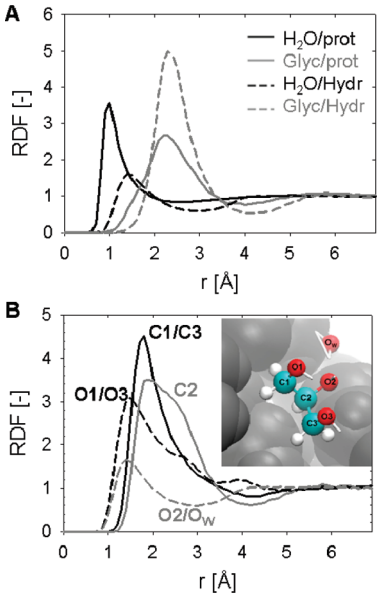

FIGURE 7: Radial distribution functions (RDFs) of (A) the centers of mass of water and glycerol at the protein surface and at a hydrophobic surface and (B) C and O atoms of water and glycerol with respect to a hydrophobic surface. Atom RDFs indicate that glycerol prefers orientations in which C atoms make contact with the protein surface and O atoms point toward the solvent, similar to the glycerol orientation in the inset.

protein surface. Besides, characteristic residence times at the hydrophobic surface are considerably longer for glycerol (1.85 ns) than for water (0.13 ns). Thus, the picture in which glycerol acts as an energetically favorable amphiphilic interface between the hydrophobic surface and polar solvent atoms arises.

This picture qualitatively agrees with the transfer free energy of CH_2 groups for transfer from pure water to aqueous glycerol which is characterized by favorable enthalpic contributions that outweigh unfavorable entropic contributions (*70*). Preferential interaction of glycerol with hydrophobic surfaces is also evident from the negative transfer free energy for transfer of toluene from pure water to glycerol/water mixtures (*71*) and the decrease in the surface tension of water by glycerol (*23*). In contrast, glycerol is preferentially excluded from native proteins (*38*), and the excess enthalpy of transfer of HEL from pure water to 30% (v/v) glycerol/water mixtures is unfavorable (*72*). Interestingly, glycerol is also preferentially excluded from hydrophobically modified cellulose (*73*). Moreover, the preferential hydration of glycerol does not correlate with the protein hydrophobicity (*38*), and no preferential interaction of glycerol is observed at protein surface regions with few polar atoms (*53*). These observations suggest that a limited amount of polar atoms prevents preferential interactions of glycerol with hydrophobic surfaces.

Further insight into preferential interactions of glycerol with hydrophobic surfaces is obtained by comparing local concentration maps for water and glycerol for HEL and for the hydrophobic surface with the same topology (Figure 8). Such local concentration maps show solvent regions that are preferentially hydrated and solvated (*53*). Preferentially hydrated solvent regions occur only at the protein surface and not at the hydrophobic surface, but preferentially solvated regions occur for both the protein surface and the hydrophobic surface and are located at depressions in the protein surface. Remarkably, preferentially solvated solvent regions differ between the protein and the hydrophobic surface in that (1) the combined volume comprised

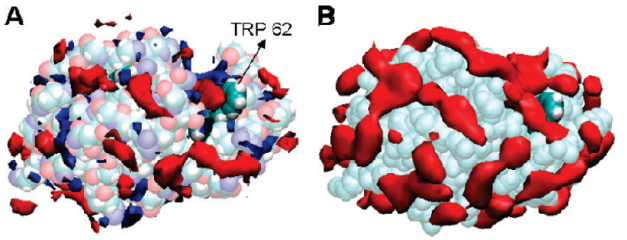

FIGURE 8: Local concentration maps for water (dark blue) and glycerol (dark red) for HEL (A; results from Sim F1) and for the hydrophobic surface with the same topology as the protein (B; results from Sim E1). Isosurfaces show the solvent regions where $g_{WP}(\vec{r}) > 1.5$ or $g_{XP}(\vec{r}) > 1.5$. Protein atoms are colored as in Figure 3, and Trp 62 is highlighted in a darker shade.

by preferentially solvated regions is considerably larger for the hydrophobic surface than for the protein surface and (2) several of these regions are located at different surface loci.

Interestingly, certain solvent regions that are preferentially solvated are located at the same surface loci of the protein and the hydrophobic surface (Figure 8). Even in such regions glycerol interactions are different for the protein and the hydrophobic surface. This is illustrated by the difference in the interactions of glycerol with the side chain of Trp62 for the protein versus the hydrophobic surface. Notably, Trp62 is located in the sugar-binding site of HEL where it is part of the largest hydrophobic region of the protein surface (*74*). For the protein, glycerol is predominantly oriented such that C atoms make contact with the side chain of Trp62 and one hydrogen bond is formed with the O atom of Asp101 (Figure 9A). However, for the hydrophobic surface, glycerol molecules populate the entire pocket between Trp62 and Asp101 where it predominantly adapts orientations whereby C atoms make contact with the hydrophobic surface and O atoms point toward the polar solvent (Figure 9B). Such orientations correspond with the amphiphilic interface orientation of glycerol at the hydrophobic surface (Figure 7B). Interactions of glycerol with the protein and the hydrophobic surface also differ for other preferentially solvated regions. This becomes evident when considering that preferentially solvated solvent regions in the local domain of HEL are located near depressions in the protein surface that consist of two or more polar protein atoms and also have affinity for water (*53*): glycerol−protein interactions at such protein loci will obviously differ from glycerol−protein interactions at the hydrophobic surface. Therefore, we conclude that native HEL lacks preferentially solvated hydrophobic surface regions that favor amphiphilic interface orientations of glycerol.

To evaluate the effects of preferential interactions of glycerol with hydrophobic surfaces on protein stability, the following questions are pertinent. What are the characteristics of preferentially solvated hydrophobic surface regions that favor amphiphilic interface orientations of glycerol? Do such hydrophobic surface regions occur for other protein conformations? We pointed out earlier that regions on the hydrophobic surface that are preferentially solvated by glycerol are located at surface depressions. Besides, the examination of glycerol−protein interactions near Trp62 shows that the mere presence of a polar protein atom in the vicinity of a hydrophobic surface region may considerably change the solvation characteristics in this region. Notably, the minimum distance between Trp62 and the O atom of Asp101 that favors hydrogen bonding with the glycerol molecule at Trp62 (Figure 9A), which is ca. 7.5 Å, gives an idea

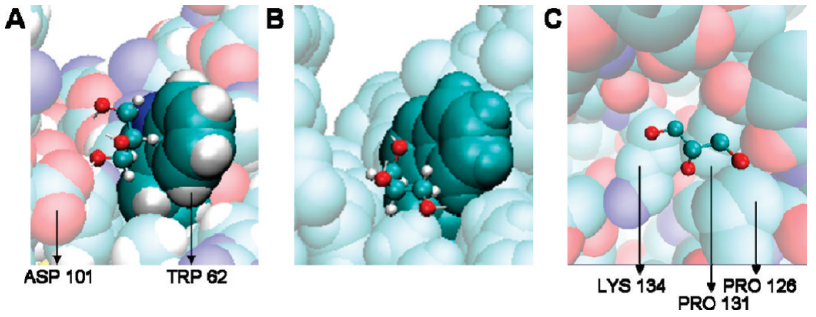

FIGURE 9: Preferred glycerol orientations at Trp62 of HEL (A; results from Sim F1), at the corresponding surface region of the hydrophobic surface with the same topology as HEL (B; results from Sim E1), and at the hydrophobic surface region formed by Pro126, Pro131, and Lys134 of Factor Xa (C; glycerol molecule resolved in PDB entry 1FJS). Glycerol and proteins are depicted as in Figure 3, and atoms of Trp62 are highlighted in a darker shade; atoms of the hydrophobic surface are uniformly colored cyan.

of the extent of the surrounding surface that might interfere with interactions between glycerol and the hydrophobic surface region. Cooperative interactions of a glycerol molecule with polar protein atoms complicate the identification of characteristics of preferentially solvated hydrophobic surface regions that favor amphiphilic interface orientations of glycerol. Identification of the characteristics of such hydrophobic surface regions is further complicated by the complex effects of the surface topology on glycerol−protein interactions. Accounting for all these effects appears to be a daunting task; nevertheless, the analysis of solvation characteristics of the hydrophobic surface with the same topology as HEL reveals that large protein surface depressions with contiguous hydrophobicity generally favor amphiphilic interface orientations of glycerol. Notably, the hydrophobic surface depression should be large enough to host amphiphilic interface orientations of glycerol without interference of neighboring polar atoms, and the topology of the depression should be such that glycerol molecules can form an interface between the hydrophobic surface and the polar solvent.

Native HEL lacks preferentially solvated hydrophobic surface regions that favor amphiphilic interface orientations of glycerol. Examination of glycerol molecules resolved in two protein crystal structures indicates that such glycerol orientations are also unusual for other native proteins: of a total of 12 glycerol molecules resolved in PDB entries 1FJS and 2W40, only one glycerol molecule is oriented such that C atoms contact the hydrophobic surface region and O atoms point toward the solvent (Figure 9C); the other 11 glycerol molecules form multiple hydrogen bonds with the protein surface. This further suggests that native protein surfaces generally have few or no hydrophobic surface regions that favor amphiphilic interface orientations of glycerol, and therefore, the contribution of such hydrophobic surface regions to Γ_{XP} values of native proteins will be minimal.

The strongly positive value of Γ_{XP} for Sim E1 [38.5 ± 1.1 (Table 1)] indicates the strong preferential solvation of hydrophobic surface regions that favor amphiphilic interface orientations of glycerol. Hence, Γ_{XP} would increase significantly as a result of protein conformational changes, leading to the creation of such hydrophobic surface regions. Protein conformations sampled in our simulations are mostly nativelike, and we do not observe such hydrophobic regions; however, it is conceivable that such hydrophobic regions occur for non-native protein conformations. The occurrence of such hydrophobic regions is most probable for protein conformations with large patches of contiguous surface hydrophobicity. In contrast to the native and unfolded conformations in which hydrophobic side chains are scattered relatively randomly in many small hydrophobic regions, protein conformations with large patches of contiguous surface hydrophobicity are prone to aggregate (*7*). Hence, we hypothesize that preferential solvation of hydrophobic regions that favor amphiphilic interface orientations of glycerol generally leads to an increase in Γ_{XP} for aggregation-prone intermediates with respect to the native and the totally unfolded state.

Aggregation-prone protein folding intermediates are not suitable for study under equilibrium, and therefore, Γ_{XP} values of such intermediates cannot be measured. Moreover, the lack of atomic-level structures of aggregation-prone protein folding intermediates prohibits molecular dynamics investigations of preferential interactions of such intermediates in aqueous glycerol. Therefore, the hypothesis that preferential solvation of hydrophobic surface regions that favor amphiphilic interface orientations of glycerol generally leads to the increase in Γ_{XP} for aggregation-prone intermediates with respect to the native and the totally unfolded state cannot be verified directly. Nevertheless, this hypothesis is corroborated by its congruency with the current understanding of the structural nature of aggregation-prone protein conformations and the insight into preferential interactions of hydrophobic surface regions in aqueous glycerol.

Inhibition of Protein Aggregation. It is commonly accepted that protein aggregation occurs through (1) partial unfolding of the native protein leading to the partial exposure of the hydrophobic core and the formation of large patches of contiguous surface hydrophobicity, followed by (2) interprotein interactions of exposed hydrophobic patches leading to protein association (Figure 10) (*7*, *10*). We propose that glycerol inhibits both steps. First, glycerol prevents partial unfolding of the native protein in the same way as it induces protein compaction. This is because in the initial stages of unfolding the protein expands without significant changes in the protein surface composition. In that case, volume increments of the local domain will be preferentially hydrated and the compact native conformation is favored. However, as unfolding proceeds, large patches of contiguous hydrophobicity are exposed to the solvent. As discussed in the previous section, hydrophobic regions that favor amphiphilic interface orientations of glycerol are preferentially solvated and large patches of contiguous hydrophobicity have a high propensity to favor amphiphilic interface orientations of glycerol. Preferential solvation of such patches at the surface of aggregation-prone intermediates will stabilize partially unfolded intermediates with respect to the transition state that leads to association of these intermediates (Figure 10). Consequently, the association of partially unfolded intermediates is inhibited.

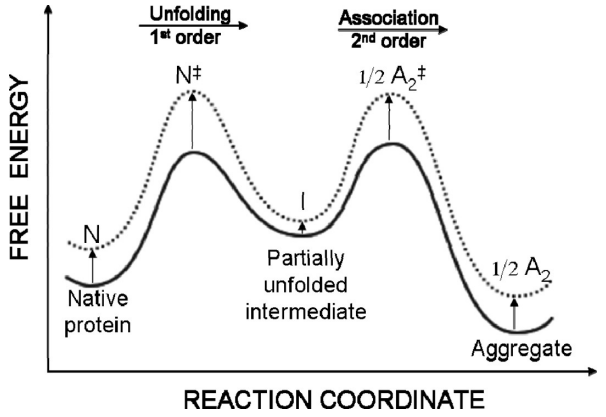

FIGURE 10: Proposed mechanisms of the inhibition of protein aggregation by glycerol. The free energy along the reaction coordinate in the absence of glycerol is shown as a solid line and in the presence of glycerol as a dashed line. Glycerol prevents partial unfolding of the native protein due to preferential hydration of the expanded transition state ($N^{\ddagger}$) compared to the native state (N). Moreover, glycerol prevents the association of aggregation-prone intermediates (I) due to preferential interactions with large patches of contiguous hydrophobicity that are buried in the protein interior for N and $N^{\ddagger}$ and form protein−protein interactions in aggregate A2 and transition state $A_2^{\ddagger}$. Although the free energy diagram represents a specific aggregation pathway, the proposed mechanisms also apply to other aggregation pathways (*95*).

Preferential solvation of large patches of contiguous hydrophobicity would decrease the free energy of aggregation-prone unfolding intermediates not only with respect to the association transition state but also with respect to the folding transition state (Figure 10). This is in accord with the stabilizing effect of glycerol on folding intermediates (*26*, *45*−*48*) and the decrease in both the aggregation rate and the folding rate (*31*, *46*) during refolding of proteins in the presence of glycerol. According to the mechanisms proposed in Figure 10, the rate of the first-order refolding reaction decreases less than the rate of the second-order association reaction. This explains why the yield of refolding increases in the presence of glycerol.

Also, the increase in the colloidal stability of HEL solutions caused by glycerol (*75*) agrees with the proposed mechanisms of glycerol-induced inhibition of protein aggregation. Moreover, glycerol reduces the level of binding of hydrophobic probes to unstable proteins (*44*, *76*). This has been attributed to the glycerol-induced rearrangement of hydrophobic surface regions into the protein interior. However, if glycerol would merely induce the burial of hydrophobic surface regions into the protein interior, glycerol would also promote the association of hydrophobic surface regions into protein aggregates. In contrast, the mechanisms proposed by us suggest that glycerol inhibits binding of hydrophobic probes by competing with hydrophobic probes to interact with the hydrophobic surface regions.

Preferential solvation of large patches of contiguous hydrophobicity in aggregation-prone intermediates inhibits protein association of such intermediates. On the other hand, preferential exclusion of glycerol from most native protein surface regions [with specific glycerol-binding loci being a notable exception (*53*)] and preferential hydration of volume increments upon protein expansion are essential for inducing conformational stability and preventing unfolding of the native protein. Our findings on the preferential interaction characteristics of glycerol and the inferred protein stabilization mechanisms prompted us to further examine (1) the extent to which these characteristics apply to other cosolvents and (2) the molecular properties of glycerol underlying these mechanisms.

Earlier, we rationalized that the mechanisms of glycerol-induced protein compaction, i.e., through preferential hydration of volume increments of the local domain due to electrostatic orientation of glycerol at the protein surface and due to the excluded volume effect, also apply to other polyols. The proposed mechanism for the inhibition of the association of aggregation-prone intermediates, i.e., stabilization of aggregation-prone intermediates through preferential solvation of hydrophobic surface regions that favor amphiphilic interface orientations of the cosolvent, is also congruent with experimental data of protein refolding in the presence of polyols other than glycerol. For example, Dong et al. (*77*) showed that protein−protein interactions of partially denatured HEL intermediates become more repulsive in the presence of trehalose. Remarkably, the effects of trehalose on protein−protein interactions of native HEL and fully denatured HEL are less pronounced. These results agree with the proposed mechanism for glycerol-induced inhibition of protein association due to the stabilization of partially unfolded intermediates with hydrophobic surface regions that favor amphiphilic interface orientations of glycerol. However, further research is needed to confirm the validity of this mechanism for other polyols.

In contrast to glycerol, more hydrophobic cosolvents such as ethanol preferentially interact with native hydrophobic surface regions (*78*) and decrease the conformational stability (*78*, *79*). Interestingly, also ethylene glycol, with a hydrophobicity is comparable to that of glycerol, decreases the conformational stability for many (but not all) proteins (*15*, *79*, *80*). Since ethylene glycol is smaller than glycerol, a reduced but nevertheless stabilizing effect is expected due to preferential hydration of volume increments of the local domain. We propose that destabilization by ethylene glycol occurs for native proteins with a relatively high surface coverage of hydrophobic surface regions that are large enough to favor amphiphilic interface orientations of ethylene glycol. In that case, protein expansion would be favored as the gain in Γ_{XP} due to preferential solvation of these hydrophobic surface regions will offset the decrease in Γ_{XP} due to preferential hydration of other surface regions. Moreover, we expect that most of the hydrophobic surface regions that are preferentially solvated by ethylene glycol will not be preferentially solvated by glycerol as they would be too small to favor amphiphilic interface orientations of glycerol. This suggests that the molecular size of the cosolvent critically affects preferential interactions with hydrophobic surfaces.

Other cosolvents such as polyethylene glycols and arginine also preferentially interact with certain hydrophobic regions (*81*, *82*). Although they do not considerably enhance the conformational stability of native proteins, they can stabilize partially unfolded intermediates (*32*, *82*) and can be effective aggregation inhibitors during refolding (*31*, *32*, *81*−*83*). Similarly, various linear di- and polyamines (*84*, *85*) and amino acid esters (*86*) inhibit protein aggregation without enhancing the conformational stability of the native protein. All these cosolvents are comprised of adjacent C atoms surrounded by polar atoms. We propose that like glycerol, such cosolvents preferentially interact with hydrophobic surface regions through the formation of amphiphilic interfaces and therefore inhibit the association of aggregation-prone intermediates.

Also, the protein denaturant urea preferentially interacts with hydrophobic surface regions of small solutes and proteins (*87*−*90*). At nondenaturing concentrations (< 2 M), urea is widely used to inhibit aggregation during refolding and is known

to improve the refolding yield for many (but not all) proteins (*32*, *91*, *92*). This effect which is attributed to a strong deceleration of aggregation as compared to folding (*32*) can be explained by the same mechanism as glycerol-induced inhibition of protein association. However, different from glycerol, urea also preferentially interacts with backbone polar groups and charged side chains of the protein surface and has a destabilizing effect on the native protein state (*87*, *89*, *90*). Depending on the nature of the changes in the protein surface along the aggregation pathway, this destabilizing effect might outdo the stabilizing effect due to preferential interactions of urea with hydrophobic surface regions. Hence, effects of urea on protein refolding will depend on the surface characteristics of the folding intermediates.

The discussion given above suggests that several cosolvents may inhibit the association of aggregation-prone intermediates through preferential interactions with hydrophobic surface regions that favor amphiphilic interface orientations of the cosolvent. The effectiveness of this effect will depend on both the affinity of hydrophobic surface regions for the hydrophobic cosolvent interface and the polarity of the cosolvent interface presented to the solvent. The importance of both the hydrophobicity and polarity of a cosolvent to inhibit protein aggregation was evidenced by Hirano et al. (*93*). Unfortunately, simple metrics for preferential interactions of cosolvents with hydrophobic protein surface regions such as the cosolvent-induced change in the solubility of hydrophobic amino acids (*93*) or the cosolvent-induced change in the surface tension (*38*) are of limited scope. The deficiency of such metrics is commonly attributed to the specific dependency of cosolvent−protein interactions on the physicochemical characteristics of both the cosolvent and the protein surface (*16*, *41*). This specificity advocates for the comprehensive characterization of local solvent−protein interactions in understanding how cosolvents affect protein thermodynamics and protein aggregation. If accurate force field parameters and relevant protein structures are available, this can be achieved by molecular dynamics simulations.

CONCLUSIONS

In this study, we have derived mechanisms of glycerol-induced protein stabilization by combining the thermodynamic framework of preferential interactions with molecular-level insight into solvent−protein interactions. A series of 40 ns molecular dynamics simulations for lysozyme in aqueous glycerol have shown that conformational changes in the protein backbone result in significant differences in the preferential interaction coefficient. Two mechanisms underlying such differences have been identified: (1) the creation or deletion of glycerol-binding loci at the protein surface by specific reorientation of protein N and O atoms that favor the formation of multiple hydrogen bonds with glycerol and (2) preferential hydration of volume increments of the local domain near the protein surface.

The first mechanism is responsible for specific changes in the protein energy surface; the second mechanism causes the overall shift of the native protein ensemble toward more compact conformations. Contrary to the common conception that protein compaction and stabilization by polyols are governed by the molecular size of the polyol, glycerol-induced protein compaction mainly originates from electrostatic interactions that induce orientations of glycerol molecules at the protein surface such that glycerol is further excluded. Furthermore, we propose that to understand protein compaction and stabilization by other polyols, the molecular size and orientation of polyol molecules at the protein surface should be taken into account.

Large protein surface depressions with contiguous hydrophobicity that favor amphiphilic interface orientations of glycerol are preferentially solvated. Such hydrophobic surface regions are expected for aggregation-prone intermediates but not for other protein conformations, and we argue that preferential solvation of hydrophobic surface regions that favor amphiphilic interface orientations of glycerol generally leads to an increase in Γ_{XP} for aggregation-prone intermediates with respect to other protein conformations. Accordingly, we propose that glycerol prevents protein aggregation by inhibiting protein unfolding and by stabilizing aggregation-prone partially unfolded intermediates through preferential interactions with hydrophobic surface regions that favor amphiphilic interface orientations of glycerol. Preferential interactions with hydrophobic surface regions also occur for other cosolvents, including arginine and urea. However, in contrast to glycerol, most of these cosolvents also preferentially interact with hydrophobic surface regions of the native protein. Consequently, they do not stabilize native proteins.

Preferential interaction characteristics of glycerol with the protein surface, i.e., preferential interactions with glycerol-binding loci and hydrophobic surface regions that favor amphiphilic interface orientations of glycerol, but preferential exclusion from other surface regions, arise from the subtle and complex balance of local physicochemical characteristics of the protein and the cosolvent. Therefore, molecular-level characterization of solvent−protein interactions is desired for the comprehension of the effects of cosolvents on protein structure and stability. As demonstrated in this study, molecular-level understanding of mechanisms of the effects of cosolvents on protein structure and stability can be obtained from molecular simulations combined with preferential interaction theory.

ACKNOWLEDGMENT

We acknowledge A*Star Computational Resource Centre for computational resources and technical assistance.

SUPPORTING INFORMATION AVAILABLE

Simulation details, figures showing the proportionality of the number of solvent molecules in the local domain with respect to the volume of the local domain, and figures showing that conformational changes are nativelike and significantly affect Γ_{XP} by two distinct mechanisms. This material is available free of charge via the Internet at http://pubs.acs.org.

REFERENCES

1. Timasheff, S. N. (1998) Control of protein stability and reactions by weakly interacting cosolvents: The simplicity of the complicated. *Adv. Protein Chem. 51*, 355–432.
2. Collins, K. D. (2004) Ions from the Hofmeister series and osmolytes: Effects on proteins in solution and in the crystallization process. *Methods 34*, 300–311.
3. Kamerzell, T. J., and Middaugh, C. R. (2008) The complex interrelationships between protein flexibility and stability. *J. Pharm. Sci. 97*, 3494–3517.
4. Chi, E. Y., Krishnan, S., Kendrick, B. S., Chang, B. S., Carpenter, J. F., and Randolph, T. W. (2003) Roles of conformational stability and colloidal stability in the aggregation of recombinant human granulocyte colony-stimulating factor. *Protein Sci. 12*, 903–913.
5. Chi, E. Y., Krishnan, S., Randolph, T. W., and Carpenter, J. F. (2003) Physical stability of proteins in aqueous solution: Mechanism and

driving forces in nonnative protein aggregation. *Pharm. Res. 20*, 1325–1336.
6. Wang, W. (2005) Protein aggregation and its inhibition in biopharmaceutics. *Int. J. Pharm. 289*, 1–30.
7. Fink, A. L. (1998) Protein aggregation: Folding aggregates, inclusion bodies and amyloid. *Folding Des. 3*, R9–R23.
8. Frokjaer, S., and Otzen, D. E. (2005) Protein drug stability: A formulation challenge. *Nat. Rev. Drug Discovery 4*, 298–306.
9. McClements, D. J. (2002) Modulation of globular protein functionality by weakly interacting cosolvents. *Crit. Rev. Food Sci. Nutr. 42*, 417–471.
10. Cellmer, T., Bratko, D., Prausnitz, J. M., and Blanch, H. W. (2007) Protein aggregation in silico. *Trends Biotechnol. 25*, 254–261.
11. Henzler-Wildman, K., and Kern, D. (2007) Dynamic personalities of proteins. *Nature 450*, 964–972.
12. Reichmann, D., Rahat, O., Cohen, M., Neuvirth, H., and Schreiber, G. (2007) The molecular architecture of protein-protein binding sites. *Curr. Opin. Struct. Biol. 17*, 67–76.
13. Frauenfelder, H., Fenimore, P. W., Chen, G., and McMahon, B. H. (2006) Protein folding is slaved to solvent motions. *Proc. Natl. Acad. Sci. U.S.A. 103*, 15469–15472.
14. Frauenfelder, H., Sligar, S. G., and Wolynes, P. G. (1991) The Energy Landscapes and Motions of Proteins. *Science 254*, 1598–1603.
15. Gekko, K., and Morikawa, T. (1981) Thermodynamics of Polyol-Induced Thermal Stabilization of Chymotrypsinogen. *J. Biochem. 90*, 51–60.
16. Kaushik, J. K., and Bhat, R. (1998) Thermal stability of proteins in aqueous polyol solutions: Role of the surface tension of water in the stabilizing effect of polyols. *J. Phys. Chem. B 102*, 7058–7066.
17. Haque, I., Singh, R., Moosavi-Movahedi, A. A., and Ahmad, F. (2005) Effect of polyol osmolytes on ΔG(D), the Gibbs energy of stabilisation of proteins at different pH values. *Biophys. Chem. 117*, 1–12.
18. Kim, Y. S., Jones, L. S., Dong, A. C., Kendrick, B. S., Chang, B. S., Manning, M. C., Randolph, T. W., and Carpenter, J. F. (2003) Effects of sucrose on conformational equilibria and fluctuations within the native-state ensemble of proteins. *Protein Sci. 12*, 1252–1261.
19. Cioni, P., Bramanti, E., and Strambini, G. B. (2005) Effects of sucrose on the internal dynamics of azurin. *Biophys. J. 88*, 4213–4222.
20. Priev, A., Almagor, A., Yedgar, S., and Gavish, B. (1996) Glycerol decreases the volume and compressibility of protein interior. *Biochemistry 35*, 2061–2066.
21. Scharnagl, C., Reif, M., and Friedrich, J. (2005) Stability of proteins: Temperature, pressure and the role of the solvent. *Biochim. Biophys. Acta 1749*, 187–213.
22. Gregory, R. B. (1988) The Influence of Glycerol on Hydrogen Isotope Exchange in Lysozyme. *Biopolymers 27*, 1699–1709.
23. Chanasattru, W., Decker, E. A., and McClements, D. J. (2008) Impact of cosolvents (polyols) on globular protein functionality: Ultrasonic velocity, density, surface tension and solubility study. *Food Hydrocolloids 22*, 1475–1484.
24. Davis-Searles, P. R., Morar, A. S., Saunders, A. J., Erie, D. A., and Pielak, G. J. (1998) Sugar-induced molten-globule model. *Biochemistry 37*, 17048–17053.
25. Timasheff, S. N. (1993) The Control of Protein Stability and Association by Weak-Interactions with Water: How Do Solvents Affect These Processes? *Annu. Rev. Biophys. Biomol. Struct. 22*, 67–97.
26. Mishra, R., Bhat, R., and Seckler, R. (2007) Chemical chaperone-mediated protein folding: Stabilization of P22 tailspike folding intermediates by glycerol. *Biol. Chem. 388*, 797–804.
27. Lee, J. C., and Timasheff, S. N. (1977) Invitro Reconstitution of Calf Brain Microtubules: Effects of Solution Variables. *Biochemistry 16*, 1754–1764.
28. Kornblatt, J. A., Kornblatt, M. J., Hoa, G. H. B., and Mauk, A. G. (1993) Responses of 2 Protein-Protein Complexes to Solvent Stress: Does Water Play a Role at the Interface? *Biophys. J. 65*, 1059–1065.
29. Goldbaum, F. A., Schwarz, F. P., Eisenstein, E., Cauerhff, A., Mariuzza, R. A., and Poljak, R. J. (1996) The effect of water activity on the association constant and the enthalpy of reaction between lysozyme and the specific antibodies D1.3 and D44.1. *J. Mol. Recognit. 9*, 6–12.
30. Xavier, K. A., Shick, K. A., SmithGill, S. J., and Willson, R. C. (1997) Involvement of water molecules in the association of monoclonal antibody HyHEL-5 with bobwhite quail lysozyme. *Biophys. J. 73*, 2116–2125.
31. Mishra, R., Seckler, R., and Bhat, R. (2005) Efficient refolding of aggregation-prone citrate synthase by polyol osmolytes: How well are protein folding and stability aspects coupled? *J. Biol. Chem. 280*, 15553–15560.
32. Clark, E. D., Schwarz, E., and Rudolph, R. (1999) Inhibition of aggregation side reactions during in vitro protein folding. *Methods Enzymol. 309*, 217–236.
33. Buckle, A. M., Devlin, G. L., Jodun, R. A., Fulton, K. F., Faux, N., Whisstock, J. C., and Bottomley, S. P. (2005) The matrix refolded. *Nat. Methods 2*, 3.
34. Qoronfleh, M. W., Hesterberg, L. K., and Seefeldt, M. B. (2007) Confronting high-throughput protein refolding using high pressure and solution screens. *Protein Expression Purif. 55*, 209–224.
35. Fields, P. A., Wahlstrand, B. D., and Somero, G. N. (2001) Intrinsic versus extrinsic stabilization of enzymes: The interaction of solutes and temperature on A(4)-lactate dehydrogenase orthologs from warm-adapted and cold-adapted marine fishes. *Eur. J. Biochem. 268*, 4497–4505.
36. Meng, F. G., Hong, Y. K., He, H. W., Lyubarev, A. E., Kurganov, B. I., Yan, Y. B., and Zhou, H. M. (2004) Osmophobic effect of glycerol on irreversible thermal denaturation of rabbit creatine kinase. *Biophys. J. 87*, 2247–2254.
37. Gangadhara, Kumar, P., and Prakash, V. (2008) Influence of Polyols on the Stability and Kinetic Parameters of Invertase from *Candida utilis*: Correlation with the Conformational Stability and Activity. *Protein J. 27*, 440–449.
38. Gekko, K., and Timasheff, S. N. (1981) Mechanism of Protein Stabilization by Glycerol: Preferential Hydration in Glycerol-Water Mixtures. *Biochemistry 20*, 4667–4676.
39. Davis-Searles, P. R., Saunders, A. J., Erie, D. A., Winzor, D. J., and Pielak, G. J. (2001) Interpreting the effects of small uncharged solutes on protein-folding equilibria. *Annu. Rev. Biophys. Biomol. Struct. 30*, 271–306.
40. Bolen, D. W. (2004) Effects of naturally occurring osmolytes on protein stability and solubility: Issues important in protein crystallization. *Methods 34*, 312–322.
41. Tiwari, A., and Bhat, R. (2006) Stabilization of yeast hexokinase A by polyol osmolytes: Correlation with the physicochemical properties of aqueous solutions. *Biophys. Chem. 124*, 90–99.
42. Feng, S., and Yan, Y. B. (2008) Effects of glycerol on the compaction and stability of the wild type and mutated rabbit muscle creatine kinase. *Proteins: Struct., Funct., Bioinf. 71*, 844–854.
43. Sedgwick, H., Cameron, J. E., Poon, W. C. K., and Egelhaaf, S. U. (2007) Protein phase behavior and crystallization: Effect of glycerol. *J. Chem. Phys. 127*, 125102.
44. Sahu, R. K., and Prakash, V. (2008) Mechanism of prevention of aggregation of proteins: A case study of aggregation of α-globulin in glycerol. *Int. J. Food Prop. 11*, 613–623.
45. Knubovets, T., Osterhout, J. J., Connolly, P. J., and Klibanov, A. M. (1999) Structure, thermostability, and conformational flexibility of hen egg-white lysozyme dissolved in glycerol. *Proc. Natl. Acad. Sci. U. S.A. 96*, 1262–1267.
46. Wu, L. Z., Ma, B. L., Sheng, Y. B., and Wang, W. (2008) Equilibrium and kinetic analysis on the folding of hen egg lysozyme in the aqueous-glycerol solution. *J. Mol. Struct. 891*, 167–172.
47. Raibekas, A. A., and Massey, V. (1996) Glycerol-induced development of catalytically active conformation of *Crotalus adamanteus* L-amino acid oxidase in vitro. *Proc. Natl. Acad. Sci. U.S.A. 93*, 7546–7551.
48. Kamiyama, T., Sadahide, Y., Nogusa, Y., and Gekko, K. (1999) Polyol-induced molten globule of cytochrome c: An evidence for stabilization by hydrophobic interaction. *Biochim. Biophys. Acta 1434*, 44–57.
49. Grudzielanek, S., Jansen, R., and Winter, R. (2005) Solvational tuning of the unfolding, aggregation and amyloidogenesis of insulin. *J. Mol. Biol. 351*, 879–894.
50. Timasheff, S. N. (2002) Protein hydration, thermodynamic binding, and preferential hydration. *Biochemistry 41*, 13473–13482.
51. Pierce, V., Kang, M., Aburi, M., Weerasinghe, S., and Smith, P. E. (2008) Recent applications of Kirkwood-Buff theory to biological systems. *Cell Biochem. Biophys. 50*, 1–22.
52. Shimizu, S., and Boon, C. L. (2004d) The Kirkwood-Buff theory and the effect of cosolvents on biochemical reactions. *J. Chem. Phys. 121*, 9147–9155.
53. Vagenende, V., Yap, M. G. S., and Trout, B. L. (2009) Molecular anatomy of preferential interaction coefficients by elucidating protein solvation in mixed solvents: Methodology and application for lysozyme in aqueous glycerol. *J. Phys. Chem. B 113*, 11743–11753.
54. Courtenay, E. S., Capp, M. W., Anderson, C. F., and Record, M. T. (2000) Vapor pressure osmometry studies of osmolyte-protein interactions: Implications for the action of osmoprotectants in vivo and for the interpretation of "osmotic stress" experiments in vitro. *Biochemistry 39*, 4455–4471.

55. Schneider, C. P., and Trout, B. L. (2009) Investigation of Cosolute-Protein Preferential Interaction Coefficients: New Insight into the Mechanism by Which Arginine Inhibits Aggregation. *J. Phys. Chem. B 113*, 2050–2058.
56. Xie, G. F., and Timasheff, S. N. (1997) Mechanism of the stabilization of ribonuclease A by sorbitol: Preferential hydration is greater for the denatured than for the native protein. *Protein Sci. 6*, 211–221.
57. Diwakar, S., Shinde, C., and Trout, B. L. (2009) Molecular computations of preferential interaction coefficients of proteins. *J. Phys. Chem. B 113*, 12546–12554.
58. Brooks, B. R., Bruccoleri, R. E., Olafson, B. D., States, D. J., Swaminathan, S., and Karplus, M. (1983) Charmm: A Program for Macromolecular Energy, Minimization, and Dynamics Calculations. *J. Comput. Chem. 4*, 187–217.
59. Phillips, J. C., Braun, R., Wang, W., Gumbart, J., Tajkhorshid, E., Villa, E., Chipot, C., Skeel, R. D., Kale, L., and Schulten, K. (2005) Scalable molecular dynamics with NAMD. *J. Comput. Chem. 26*, 1781–1802.
60. Schellman, J. A. (2003) Protein stability in mixed solvents: A balance of contact interaction and excluded volume. *Biophys. J. 85*, 108–125.
61. Baynes, B. M., and Trout, B. L. (2003) Proteins in mixed solvents: A molecular-level perspective. *J. Phys. Chem. B 107*, 14058–14067.
62. To, E. C. H., Davies, J. V., Tucker, M., Westh, P., Trandum, C., Suh, K. S. H., and Koga, Y. (1999) Excess chemical potentials, excess partial molar enthalpies, entropies, volumes, and isobaric thermal expansivities of aqueous glycerol at 25 °C. *J. Solution Chem. 28*, 1137–1157.
63. Marcus, Y. (2000) Some thermodynamic and structural aspects of mixtures of glycerol with water. *Phys. Chem. Chem. Phys. 2*, 4891–4896.
64. Schwalbe, H., Grimshaw, S. B., Spencer, A., Buck, M., Boyd, J., Dobson, C. M., Redfield, C., and Smith, L. J. (2001) A refined solution structure of hen lysozyme determined using residual dipolar coupling data. *Protein Sci. 10*, 677–688.
65. Vaney, M. C., Maignan, S., RiesKautt, M., and Ducruix, A. (1996) High-resolution structure (1.33 angstrom) of a HEW lysozyme tetragonal crystal grown in the APCF apparatus. Data and structural comparison with a crystal grown under microgravity from SpaceHab-01 mission. *Acta Crystallogr. D52*, 505–517.
66. Vendruscolo, M., and Dobson, C. M. (2005) Towards complete descriptions of the free-energy landscapes of proteins. *Philos. Trans. R. Soc. London, Ser. A 363*, 433–450.
67. O'Connor, T. F., Debenedetti, P. G., and Carbeck, J. D. (2007) Stability of proteins in the presence of carbohydrates: Experiments and modeling using scaled particle theory. *Biophys. Chem. 127*, 51–63.
68. Street, T. O., Bolen, D. W., and Rose, G. D. (2006) A molecular mechanism for osmolyte-induced protein stability. *Proc. Natl. Acad. Sci. U.S.A. 103*, 13997–14002.
69. Lakshmikanth, G. S., and Krishnamoorthy, G. (1999) Solvent-exposed tryptophans probe the dynamics at protein surfaces. *Biophys. J. 77*, 1100–1106.
70. Sinha, R., Bhattacharya, S. K., and Kundu, K. K. (2005) Chemical transfer energetics of the -CH_2- group in aqueous glycerol: Solvent effect on hydrophobic hydration and its three-dimensional structure. *J. Mol. Liq. 122*, 95–103.
71. Carrillo-Nava, E., Dohnal, V., and Costas, M. (2004) Modeling Gibbs energies of solution for a non-polar solute in aqueous solutions of the protein stabilizers glycerol and ethylene glycol. *Biophys. Chem. 107*, 19–24.
72. Westh, P., and Koga, Y. (1997) Intermolecular interactions of lysozyme and small alcohols: A calorimetric investigation. *J. Phys. Chem. B 101*, 5755–5758.
73. Stanley, C., and Rau, D. C. (2008) Assessing the interaction of urea and protein-stabilizing osmolytes with the nonpolar surface of hydroxypropylcellulose. *Biochemistry 47*, 6711–6718.
74. Cheetham, J. C., Artymiuk, P. J., and Phillips, D. C. (1992) Refinement of an Enzyme Complex with Inhibitor Bound at Partial Occupancy: Hen Egg-White Lysozyme and Tri-N-acetylchitotriose at 1.75-Å Resolution. *J. Mol. Biol. 224*, 613–628.
75. Liu, W., Bratko, D., Prausnitz, J. M., and Blanch, H. W. (2004) Effect of alcohols on aqueous lysozyme-lysozyme interactions from static light-scattering measurements. *Biophys. Chem. 107*, 289–298.
76. Raibekas, A. A., and Massey, V. (1997) Glycerol-assisted restorative adjustment of flavoenzyme conformation perturbed by site-directed mutagenesis. *J. Biol. Chem. 272*, 22248–22252.
77. Dong, X. Y., Liu, J. H., Liu, F. F., and Sun, Y. (2009) Self-interaction of native and denatured lysozyme in the presence of osmolytes, L-arginine and guanidine hydrochloride. *Biochem. Eng. J. 43*, 321–326.
78. Avdulov, N. A., Chochina, S. V., Daragan, V. A., Schroeder, F., Mayo, K. H., and Wood, W. G. (1996) Direct binding of ethanol to bovine serum albumin: A fluorescent and C-13 NMR multiplet relaxation study. *Biochemistry 35*, 340–347.
79. Herskovits, T., Gadegbeku, B., and Jaillet, H. (1970) On the Structural Stability and Solvent Denaturation of Proteins. I. Denaturation by the Alcohols and Glycols. *J. Biol. Chem. 245*, 2588–2598.
80. Fujita, Y., and Noda, Y. (1984) The Effect of Ethylene-Glycol on the Thermal-Denaturation of Ribonuclease-a and Chymotrypsinogen-a as Measured by Differential Scanning Calorimetry. *Bull. Chem. Soc. Jpn. 57*, 2177–2183.
81. Ishibashi, M., Tsumoto, K., Tokunaga, M., Ejima, D., Kita, Y., and Arakawa, T. (2005) Is arginine a protein-denaturant? *Protein Expression Purif. 42*, 1–6.
82. Cleland, J. L., Builder, S. E., Swartz, J. R., Winkler, M., Chang, J. Y., and Wang, D. I. C. (1992) Polyethylene-Glycol Enhanced Protein Refolding. *Bio/Technology 10*, 1013–1019.
83. Cleland, J. L., Hedgepeth, C., and Wang, D. I. C. (1992) Polyethylene-Glycol Enhanced Refolding of Bovine Carbonic Anhydrase-B: Reaction Stoichiometry and Refolding Model. *J. Biol. Chem. 267*, 13327–13334.
84. Kudou, M., Shiraki, K., Fujiwara, S., Imanaka, T., and Takagi, M. (2003) Prevention of thermal inactivation and aggregation of lysozyme by polyamines. *Eur. J. Biochem. 270*, 4547–4554.
85. Okanojo, M., Shiraki, K., Kudou, M., Nishikori, S., and Takagi, M. (2005) Diamines prevent thermal aggregation and inactivation of lysozyme. *J. Biosci. Bioeng. 100*, 556–561.
86. Shiraki, K., Kudou, M., Sakamoto, R., Yanagihara, I., and Takagi, M. (2005) Amino acid esters prevent thermal inactivation and aggregation of lysozyme. *Biotechnol. Prog. 21*, 640–643.
87. Stumpe, M. C., and Grubmuller, H. (2008) Polar or Apolar: The Role of Polarity for Urea-Induced Protein Denaturation. *PLoS Comput. Biol.,* 4.
88. Lee, M. E., and van der Vegt, N. F. A. (2006) Does urea denature hydrophobic interactions? *J. Am. Chem. Soc. 128*, 4948–4949.
89. Hua, L., Zhou, R. H., Thirumalai, D., and Berne, B. J. (2008) Urea denaturation by stronger dispersion interactions with proteins than water implies a 2-stage unfolding. *Proc. Natl. Acad. Sci. U.S.A. 105*, 16928–16933.
90. Rossky, P. J. (2008) Protein denaturation by urea: Slash and bond. *Proc. Natl. Acad. Sci. U.S.A. 105*, 16825–16826.
91. Singh, S. M., and Panda, A. K. (2004) Solubilization and refolding of bacterial inclusion body proteins. In Annual Meeting of the Society of Biotechnology , pp 303−310, Nagoya, Japan.
92. Clark, E. D. (2001) Protein refolding for industrial processes. *Curr. Opin. Biotechnol. 12*, 202–207.
93. Hirano, A., Hamada, H., and Shiraki, K. (2008) trans-Cyclohexanediamines prevent thermal inactivation of protein: Role of hydrophobic and electrostatic interactions. *Protein J. 27*, 253–257.
94. Spinozzi, F., Ortore, M. G., Sinibaldi, R., Mariani, P., Esposito, A., Cinelli, S., and Onori, G. (2008) Microcalorimetric study of thermal unfolding of lysozyme in water/glycerol mixtures: An analysis by solvent exchange model. *J. Chem. Phys. 129*, 9.
95. Roberts, C. J. (2007) Non-native protein aggregation kinetics. *Biotechnol. Bioeng. 98*, 927–938.